information about the sparse spectrum of excited states below the emission threshold at 2.7 eV. It may be that after impact imparts energy into the vibrational degrees of freedom, leaving the electrons initially in the ground state, the rate-limiting step is the vibration-to-electronic excitation process. In this case, the appropriate prefactor is an electron-vibrational coupling constant, determined here to be near or somewhat larger than 10^8 s^{-1}. Other hypotheses have been proposed in order to account for low ionization efficiencies of large molecules (*17*).

To establish the nature of a rate process, and thereby to obtain a correct microscopic theory, it is necessary to measure the rate as a function of energy or temperature. In this report we have presented this crucial information for delayed emission of electrons from large molecules. The generality of these conclusions, derived from experiments on negatively charged fullerenes, should be examined for other cluster and molecular systems that show thermionic emission. One very interesting question is the evolution with size toward the bulk limit (Richardson equation), which in the case of fullerenes should tend toward the properties of graphite (a semimetal), and in clusters of elements like tantalum or tungsten should tend toward the properties of the bulk metal.

REFERENCES AND NOTES

1. C. Y. Ng, *Adv. Chem. Phys.* **52**, 263 (1983).
2. C. Herring and M. H. Nichols, *Rev. Mod. Phys.* **21**, 185 (1949).
3. T. Leisner *et al.*, *Z. Phys.* **D20**, 127 (1991); A. Amrein, R. Simpson, P. A. Hackett, *J. Chem. Phys.* **95**, 1781 (1991); *ibid.* **94**, 4663 (1991).
4. C. Yeretzian and R. L. Whetten, *Z. Phys.* **D24**, 199 (1992).
5. E. E. B. Campbell, G. Ulmer, I. V. Hertel, *Phys. Rev. Lett.* **67**, 1986 (1991).
6. P. M. St. John and R. L. Whetten, *Chem. Phys. Lett.* **196**, 330 (1992); P. M. St. John, C. Yeretzian, R. L. Whetten, *J. Phys. Chem.* **96**, 9100 (1992).
7. S. Maruyama, M. Y. Lee, R. E. Haufler, Y. Chai, R. E. Smalley, *Z. Phys.* **D19**, 409 (1991).
8. R. F. Foster, W. Tumas, J. I. Brauman, *J. Chem. Phys.* **79**, 4644 (1983).
9. L.-S. Wang, J. Conceicao, C. Jin, R. E. Smalley, *Chem. Phys. Lett.* **182**, 5 (1991).
10. R. D. Beck, P. M. St. John, F. Diederich, R. L. Whetten, *J. Phys. Chem.* **95**, 8402 (1991).
11. R. D. Beck, P. M. St. John, M. L. Homer, R. L. Whetten, *Science* **253**, 879 (1991).
12. This value for α has to be seen as an upper bound and will be reduced somewhat when considering the parallel momentum loss and also the thermal energy content in the incident beam. Furthermore, the limit $\alpha \leq 0.5$ should only hold for the case of surface and ion composed of similar materials.
13. Only at low energies ($E_i < 50$ eV) is the collision significantly elastic, with recoil kinetic energy accounting for >10% of the impact energy: C. Yeretzian, K. Hansen, R. D. Beck, R. L. Whetten, *J. Chem. Phys.*, in press, H.-G. Busmann, Th. Lill, I. V. Hertel, *Chem. Phys. Lett.* **187**, 459 (1991).
14. R. C. Mowrey, D. W. Brenner, B. I. Dunlap, J. W. Mintmire, C. T. White, *J. Phys. Chem.* **95**, 7138 (1991).
15. On the basis of such nonexponential decays, it has even been questioned whether the assumption of an activated rate is warranted: G. Walder and O. Echt, in *Clusters and Fullerenes*, V. Kumar and E. Tosatti, Eds. (World Scientific, Singapore, in press).
16. C. E. Klots, *Chem. Phys. Lett.* **186**, 73 (1991).
17. E. W. Schlag and R. D. Levine, *J. Phys. Chem.* **96**, 10608 (1992).

18. This research was supported by the U.S. Office of Naval Research. R.L.W. and C.Y. acknowledge grants from the Packard Foundation and the Swiss National Science Foundation, respectively.

12 January 1993; accepted 9 March 1993

Van der Waals Epitaxial Growth of α-Alumina Nanocrystals on Mica

S. Steinberg, W. Ducker, G. Vigil, C. Hyukjin, C. Frank, M. Z. Tseng, D. R. Clarke, J. N. Israelachvili*

Lattice mismatch stresses, which severely restrict heteroepitaxial growth, are greatly minimized when thin alumina films are grown by means of van der Waals forces on inert mica substrates. A 10-nanometer-thick epitaxial film exhibits crystallographic sixfold symmetry, a lattice constant close to that of the basal plane [0001] of α-alumina (sapphire), and an aluminum:oxygen atomic ratio of 1:1.51 ± 0.02 (measured by x-ray photoelectron spectroscopy), again the same as for bulk sapphire. The film is free of steps and grain boundaries over large areas and appears to be an ideal model system for studying adhesion, tribology, and other surface phenomena at atomic scales.

The potential for new materials with tailored bulk, surface, and interface properties has stimulated extraordinary interest during the past 20 years, particularly in the field of ceramic materials. Ceramics have been designed with specialized physical properties for use in electronic, optical, nuclear, and structural applications (*1*). As a typical structural ceramic, sapphire (the single-crystal form of α-alumina, Al_2O_3) shows a combination of interesting properties such as great hardness, high wear resistance, chemical inertness, and high electrical resistivity. Because of its outstanding biocompatibility and high compressive strength, high-purity alumina also serves as an excellent implant material in human prosthetic devices (*2*).

These demands and other potential applications have motivated recent investigations into the correlations between composition and the electronic and surface structure of Al_2O_3 in its various phases (*3–5*). However, less progress has been made toward developing pure sapphire crystals of homogeneous (crystalline) microstructure, free of defects and with an extremely smooth surface—that is, with a mean surface roughness in the subnanometer range. In an attempt to address these issues and in consideration of the need for using oxide materials as thin films for microdevices, we investigated the possibility of epitaxially growing thin sapphire films on mica. "Breaking the mica barrier" by seeking other crystalline surfaces that can be easily prepared as thin, semitransparent layers suitable for use in the surface forces apparatus (*5–8*) could increase our understanding of adhesion, friction, and colloidal interactions.

We used the van der Waals epitaxy (VDWE) method recently developed by Koma *et al.* (*9*) for growing two-dimensional layered materials on a variety of substrate surfaces that need not be epitaxially well matched to the layers being grown. In this method, film growth is initiated by the relatively weak and nonspecific van der Waals forces between the film and saturated substrate molecules (that is, substrate surfaces having no dangling bonds), which produces unstrained films that can be grown to thicknesses of 5 to 20 nm while their intrinsic crystalline structure is preserved. Koma *et al.* (*9*) showed that the VDWE method is very effective for growing heterostructures even when the lattice mismatch between the film and substrate lattices is as high as 10%, with one reported case—$MoSe_2$ on mica—where the lattice mismatch was 58% (*10*). If extended to other metal oxide, mineral, and ceramic surfaces, the possibility of obtaining relatively thick, defect-free films with crystalline structures that are the same as in the bulk material would represent a significant improvement over conventional molecular beam epitaxy and chemical vapor–deposited coatings, which cannot produce such layers unless the film–substrate lattice mismatch is less than ~1% (*11–15*). Other growing meth-

S. Steinberg, W. Ducker, G. Vigil, J. N. Israelachvili, Department of Chemical and Nuclear Engineering, University of California, Santa Barbara, CA 93106.
C. Hyukjin and C. Frank, Department of Chemical Engineering, Stanford University, Stanford, CA 94305.
M. Z. Tseng, Department of Electrical and Computer Engineering, University of California, Santa Barbara, CA 93106.
D. R. Clarke, Materials Department, University of California, Santa Barbara, CA 93106.

*To whom correspondence should be addressed.

ods include the nucleation and growth of a crystalline film from a condensing vapor phase [vapor phase deposition (VPD)], which can also be used to produce uniformly thick films on certain substrate surfaces.

Sapphire films, 10 nm thick, were vapor-deposited on muscovite mica substrates. Mica [$KAl_2(OH)_2(Si_3AlO_{10})$] has a layered structure in which each layer is bound by van der Waals and electrostatic forces and is easily cleaved, forming flat, atomically smooth surfaces with no exposed dangling bonds. The surface crystal structure of mica (*16*) (lattice constant a_{001} = 5.2 Å) has unit triangles of oxygen atoms arranged in a sixfold symmetry. In contrast, the basal plane of sapphire (a_{0001} = 4.759 Å) exposes close-packed arrays of oxygen ions (*17*). It was therefore important to know whether van der Waals epitaxy of sapphire would occur on mica: both materials have the same symmetry and a lattice mismatch of 9%, but this system had not been studied before and it was not obvious how growth would be affected at high temperatures. The epitaxial growth was carried out in an 18-inch glass bell jar evaporation system equipped with an electron-beam source (Temescal CV-3) having the capability of feedback control and beam sweeping. Before deposition, the chamber was cryo-pumped for 24 hours at a pressure of 8 × 10^{-8} torr. The alumina source was a highly compact Al_2O_3 pellet prepared from high-purity Al_2O_3 slurries (pH 4) filtered in a die with a mechanical press operated at 14 MPa. The pellet was then sintered for 5 hours in air at 1200°C. Growth of a 10-nm-thick film of alumina was carried out at 650°C at a rate of 0.1 nm s^{-1} on freshly cleaved mica sheets ~10 mm by 10 mm. After deposition, the system was cooled to room temperature at a rate of 5°C min^{-1}.

X-ray photoelectron spectroscopy (XPS) (*18*) was used to investigate the chemical composition of the film. All of the accessible core lines—Al 2*p*, Al 2*s*, Si 2*p*, K 2*p*, O 1*s*—apparently consist of single lines characteristic of a single chemical state and are assigned binding energies corresponding to the peak maxima. Selected high-resolution spectra of Al 2*p*, Si 2*p*, and O 1*s* are shown in Fig. 1 for the VDWE film, for a single crystal of sapphire grown by VPD, and for mica heated to 650°C (before XPS measurement). It is evident that the core line attributed to Si 2*p* in mica is absent from the VDWE film spectrum, which indicates that the epilayer entirely covers the underlying mica substrate. The XPS data for all three samples are summarized in Table 1. The attenuation length values and the photo-ionization cross sections at 1254 eV that we used to compute the stoichiometry of the analyzed samples are given in (*19*, *20*). Most remarkably, the data in Table 1 show that the Al:O atomic ratio in the film, 1:1.51 ± 0.02, is virtually the same as that in bulk sapphire.

When further investigated by auger electron spectroscopy (AES), the whole area was found to be free of contaminants. In addition, the Al *LVV* region of the AES data consisted of only two peaks—at 35 and 53 eV—precisely as expected for a sapphire crystal. Furthermore, the absence of other peaks (for example, at 67 eV) indicated that no Al^{3+} had been reduced to metallic

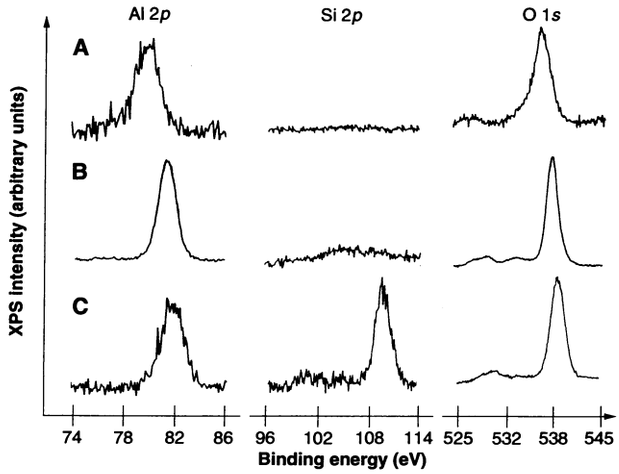

Fig. 1. High-resolution XPS core lines from a nonmonochromatic Mg ($K\alpha$ = 1254 eV) x-ray source at a take-off angle of 90° in ultrahigh vacuum (below 10^{-9} torr), detected with a concentric hemispherical analyzer at a pass energy of 50 eV for survey scans and 20 eV for high-resolution spectra. (**A**) A 10-nm-thick VDWE alumina film heteroepitaxially deposited on mica. (**B**) VPD-grown sapphire thin sheet. (**C**) Muscovite mica heated to 650°C before XPS measurement.

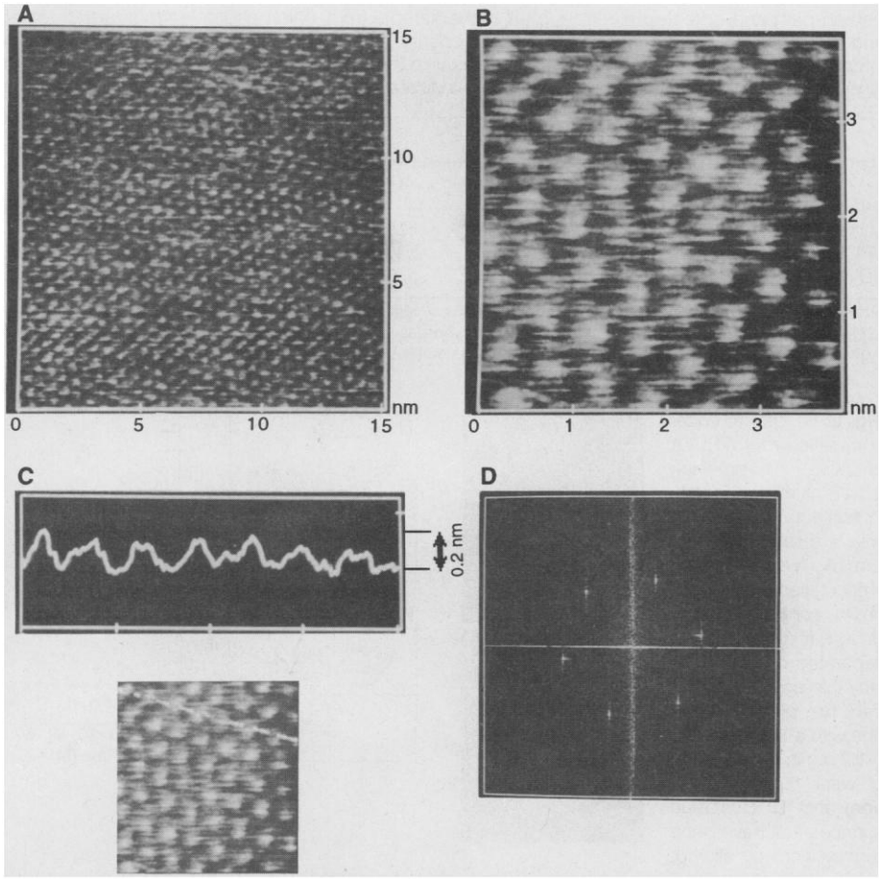

Fig. 2. AFM images of (**A**) a 15 nm by 15 nm VDWE alumina surface on mica (same surface as in Fig. 1C) and (**B**) the same surface as in (A) but at higher resolution (area is 4 nm by 4 nm). (**C**) Cross section profile through the line shown below (C), illustrating a peak-to-peak amplitude of ~0.2 nm. (**D**) Two-dimensional fast Fourier transform of image in (A). The lattice, clearly visible in both (B) and (D), was observed at various places on the film in both force and height modes and in air, water, and salt solutions and was reproducible over a period of weeks.

Al, as occurs in noncrystalline films (*21*), and that there were no Al dangling bonds at the surface (*3*).

Surface topography was determined by atomic force microscopy (AFM) with a Nanoscope II (*22*) in which a 1 μm by 1 μm scan head and a silicon nitride tip on a cantilever with a spring constant of 0.1 N m^{-1} were used. The best resolution was achieved by using the "force mode," in which the tip scans at approximately constant height and the spring deflection is measured. The images obtained are shown in Fig. 2, A and B; they are not filtered in any way and were reproducible over a period of 2 weeks. A cross section profile along the line depicted in Fig. 2C shows a peak-to-valley amplitude of ~0.2 nm, which is indicative of a highly smooth, crystallographic surface (*23*). Remarkably, the surface quality was preserved when the images were averaged over much larger scales (micrometers). We note that typical AFM topographic mapping of mica reveals similar amplitude values. The reciprocal lattice vectors (RLVs), $\mathbf{b}_n$, for typical images (such as in Fig. 2A) were determined from Fourier transforms (Fig. 2D). For three different films, the resulting wave vectors, parameterized by their magnitude b_n and the angle between adjacent RLVs $\theta_{n,n+1}$, produced values $(2\pi/b_n)$ for the lattice row repeat distance (d_n) of 0.41 ± 0.015 nm, corresponding to $a_{0001} = 0.41 \times 2/\sqrt{3} = 0.47$ ± 0.02 nm and values for θ ranging from 59.2° to 60.2° (*24*). The six Fourier spots (Fig. 2D), together with the observed values of the angle θ, are indicative of an ordered structure with hexagonal symmetry. The lattice constant values of the hexagonal unit cell, as deduced from the measurements performed on three different films, correspond within ≤3.5% to the [0001] lattice constant of the sapphire unit cell, which shows that these films grow heteroepitaxially on mica. In contrast, the lattice could not be resolved by AFM on micrometer-thick VPD films of α-alumina (*25*) grown by the VPD method described earlier and in (*26*).

Table 1. XPS data for core level photoelectrons. For constant x-ray flux, tilt angle between the photon path and detected electron, area of the sample from which photoelectrons are detected, and probability for the electron to undergo an energy loss event in addition to a plasmon loss, the intensity of a photoelectron peak (Fig. 1) scales with the number of element atoms, the attenuation length (*19*) of the photoelectron, and the photo-ionization cross section (*20*) for the sampled orbital.

Sample	Binding energy (eV)			Atomic ratios	
	Al 2*p*	Si 2*p*	O 1*s*	O:Al	Si:Al
Mica	81.99	110	539.1	4.3	1
VPD	81.43*	105.4†	538.4	1.50 ± 0.02	<0.03
VDWE	80.20*	No signal	536.8	1.51 ± 0.02	No signal

*The value of 80.20 eV for VDWE film is in good agreement with the values of 80.9 and 79.7 eV reported in (*3*) and (*21*), respectively, for sapphire single crystals, whereas for mica and VPD the values are somewhat higher. †Possible Si contamination during the deposition.

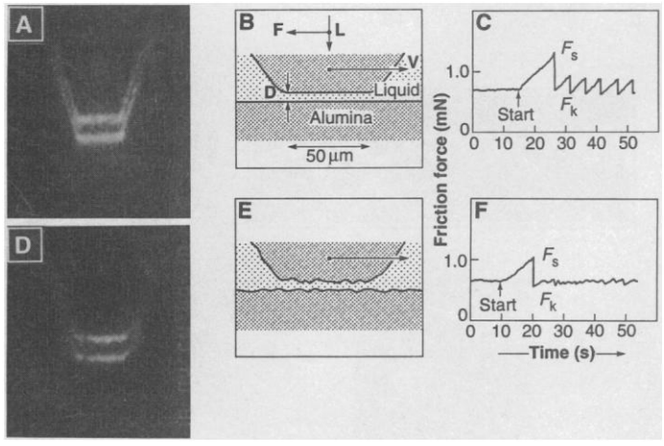

Fig. 3. Fringes of equal chromatic order (FECO) of two, 10-nm-thick VDWE alumina surfaces in contact over an area with a diameter of ~50 μm. (**A**) Two molecularly smooth surfaces in adhesive contact at rest or during frictional sliding separated by a molecularly thin boundary lubricant film of *n*-hexadecane with a thickness (*D*) ≈1.2 nm in the absence of wear (surface damage) and (**D**) crystalline surfaces that have been slightly worn by sliding, showing polycrystalline asperities of maximum height (~5 nm). (**B** and **E**) Schematic drawings of smooth and damaged surfaces, respectively, as deduced from the FECO fringe patterns in (A) and (D). (**C** and **F**) Friction traces for smooth and slightly damaged surfaces, respectively, both obtained under the same conditions of applied load and sliding speed. Note the disappearance of the regular stick-slip motion in (F), which is common for rough surfaces. Sliding velocity (**V**) = 0.2 μm s^{-1}; temperature (*T*) = 21°C; applied load (**L**) = 4 mN; and friction forces (**F**) ≈ 1.2 mN, which in the presence of stick-slip motion split up into static and kinetic components (F_s and F_k, respectively).

The combination of crystallinity, smoothness, and robustness suggested that these epilayers could function as ideal model systems for investigating various molecular-scale surface phenomena such as adhesion, friction, and colloidal interactions. We used a surface forces apparatus modified for friction studies (*27*) to measure the adhesion and interfacial friction of two VDWE alumina surfaces sliding past each other while separated by a 1.2-nm-thick film of *n*-hexadecane. The multiple beam interference fringes [fringes of equal chromatic order (FECO)] recorded during the experiments showed that the surfaces remained molecularly smooth both at rest and during sliding (Fig. 3, A and B). The friction traces indicate that under such "ideal" conditions, the sliding proceeds by means of a highly regular stick-slip motion (Fig. 3C). This shows that the hydrocarbon molecules, when confined between two structured or crystalline alumina surfaces, become ordered or solid-like and can sustain a finite shear stress (*28, 29*). In contrast, after repeated sliding over the same area, the crystalline surface lattice becomes worn (locally damaged), which is seen as small discontinuities in the FECO fringes (Fig. 3, D and E) and the regular stick-slip component of the friction disappears (Fig. 3F). Figure 3 therefore shows how nanometer-sized asperities can dramatically alter the friction of lubricated alumina surfaces.

Our findings suggest that heteroepitaxy presents a route for the construction of a variety of chemically homogeneous metal oxide surfaces that appear to retain all the advantages of the underlying mica substrate, such as transparency, atomic smoothness, and elastic flexibility. By virtue of their modified surface energy and increased susceptibility to chemical modifications as compared to mica, sapphire-like films have an obvious bearing on understanding the adhesion and molecular tribology of ceramic surfaces.

REFERENCES AND NOTES

1. L. A. Ryabova, in *Current Topics in Materials Science*, E. Kaldis, Ed. (North-Holland, Amsterdam, 1981), vol. 7, chap. 5.
2. W. Dawihl and E. Dorre, in *Evaluation of Biomaterials*, G. W. Winter, J. L. Leray, K. de Groot, Eds. (Wiley, New York, 1980), chap. 20, p. 239.
3. W. J. Gignac, R. S. Williams, S. P. Kowalczyk, *Phys. Rev. B* **32**, 1237 (1985).
4. J. Guo, D. E. Ellis, D. J. Lam, *ibid.* **45**, 13647 (1992).
5. S. J. Hirtz, A. M. Homola, G. Hadziioannou, C. W. Frank, *Langmuir* **8**, 328 (1992).
6. J. N. Israelachvili and G. E. Adams, *J. Chem. Soc. Faraday Trans. I* **74**, 975 (1978).
7. R. G. Horn, D. T. Smith, W. Haller, *Chem. Phys. Lett.* **162**, 404 (1989).
8. C. P. Smith, M. Maeda, L. Atanasoska, H. S. White, D. J. McClure, *J. Phys. Chem.* **92**, 199 (1988).
9. A. Koma, K. Sunouchi, T. Miyajima, *J. Vac. Sci. Technol.* **B3**, 724 (1985).
10. K. Ueno, K. Saiki, T. Shimada, A. Koma, *ibid.* **A8**, 68 (1990).
11. E. G. Bauer *et al.*, *J. Mater. Res.* **5**, 852 (1990).
12. H. L. M. Chang *et al.*, *ibid.* **7**, 2495 (1992).

13. A lattice mismatch bigger than 0.1% between substrate and film is thought to cause pseudomorphic growth, which results in films with crystallographic defects (*11*). In addition, the difference in the thermal expansion coefficients between epilayer and substrate produces thermal stresses at the interface (*12*).
14. H. J. Osten, J. Klatt, G. Lippert, *Appl. Phys. Lett.* **60**, 44 (1992).
15. F. S. Ohuci, B. A. Parkinson, K Ueno, A. Koma, *J. Appl. Phys.* **68**, 2168 (1990).
16. S. W. Bailey, in *Review in Minerology Micas*, S. W. Bailey, Ed. (Mineralogical Society of America, Chelsea, MI, 1984), vol. 13, chap. 2, pp. 13–60.
17. B. G. Hyde and S. Anderson, *Inorganic Crystal Structures* (Wiley, New York, 1989).
18. Vacuum Generators, ESCALAB, Center for Materials Research, Stanford University, Stanford, CA.
19. M. P. Seah and W. A. Dench, *Surf. Interface Anal.* **1**, 2 (1979).
20. J. H. Scofield, *J. Electron Spectrosc. Relat. Phenom.* **8**, 129 (1976).
21. J. Olivier and R. Poirier, *Surf. Sci.* **105**, 347 (1981).
22. Nanoscope II FM, Digital Instruments, Inc., Goleta, CA.
23. Although both the shape of the scanning tip and the interaction between tip and sample may influence the finer details of a measured image [N. A. Burnham and R. J. Colton, in *Scanning Tunneling Microscopy: Theory and Application*, D. Bonnell, Ed. (VCH Publishers, New York, 1993), chap. 7, p. 240], it is clear that the surface is very smooth and crystalline. If the recorded amplitude of 0.2 nm were artificially amplified because of such tip-substrate interactions, this would indicate that the surfaces are even smoother than the value quoted.
24. Possible systematic errors due to the calibration in the *x* and *y* directions from images of mica (*30*) are not included.
25. The higher adhesion energy measured in air between surfaces that have been prepared by VDWE as compared to the values for VPD sapphire further attest to the angstrom-scale smoothness in the former case.
26. E. A. D. White and J. D. C. Wood, *J. Mater. Sci.* **9**, 1999 (1974).
27. J. N. Israelachvili, P. M. McGuiggan, A. M. Homola, *Science* **240**, 189 (1988).
28. Recent molecular dynamic simulations with flexible linear chains trapped between two [111] planes of a face-centered-cubic lattice indicate a wall-induced glass transition of fluid films [P. A. Thompson, G. S. Grest, M. O. Robbins, *Phys. Rev. Lett.* **68**, 3448 (1992)].
29. M. L. Gee, P. M. McGuiggan, J. N. Israelachvili, *J. Chem. Phys.* **93**, 1845 (1990).
30. D. K. Schwartz, J. Garnaes, R. Viswanathan, J. A. N. Zasadzinski, *Science* **257**, 508 (1992).
31. Supported by Office of Naval Research (ONR) grant N00014-89-J-1101. We thank J. Zasadzinski for providing his AFM facility (supported by ONR grant N00014-90-J-1551) and D. Pearson, F. Lange, E. Hu, D. Schwartz, and M. Chaudhuri for helpful discussions.

30 November 1992; accepted 24 February 1993

Preparation of Amorphous Boron Nitride and Its Conversion to a Turbostratic, Tubular Form

Ewan J. M. Hamilton, Shawn E. Dolan, Charles M. Mann, Hendrik O. Colijn, Clare A. McDonald, Sheldon G. Shore*

Amorphous boron nitride, BN, is obtained from the reaction of *B*-trichloroborazine, $(BClNH)_3$, with cesium metal. The amorphous product is converted to a turbostratic form upon heating to 1100°C. Scanning electron microscopy reveals a previously unreported morphology composed of hollow tubular structures. The largest of these appear to be approximately 3 micrometers in external diameter and 50 to 100 micrometers in length. Transmission electron microscopy and selected-area electron diffraction also indicate the tube walls to be turbostratic in nature. The mechanism by which the tubes form is not known, although apparent sites of incipient tube growth have been observed.

When amorphous boron nitride (BN) obtained from the reaction between cesium and *B*-trichloroborazine ($B_3Cl_3N_3H_3$) is heated under vacuum to 1100°C, it is converted to two morphologies of turbostratic (*1*) boron nitride, a partially ordered, pseudographitic form. [A turbostratic phase of a layered material is characterized by rotational disorder in the direction normal to the layers (*1*).] In addition to the commonly observed distorted lamellar form, scanning electron microscopy (SEM) reveals the presence of hollow tubular structures, a previously unreported morphology for BN. These tubes form in a range of sizes, with diameters of approximately 3 μm and 0.15 μm being most commonly observed. High-resolution microscopy reveals that the tube walls do not possess a high degree of crystallinity but rather are turbostratic in nature.

E. J. M. Hamilton, S. E. Dolan, C. M. Mann, S. G. Shore, Department of Chemistry, Ohio State University, Columbus, OH 43210.
H. O. Colijn and C. A. McDonald, Department of Materials Science and Engineering, Ohio State University, Columbus, OH 43210.
*To whom correspondence should be addressed.

Although the mechanism of formation of this new morphology is unclear, it appears that our synthesis of the amorphous BN precursor may be a crucial factor. Traditionally, BN powders have been prepared by classical, high-temperature syntheses (*2*). These typically involve inexpensive boron- and nitrogen-bearing reagents, such as boric acid and ammonia, but complicated work-up procedures are required to obtain a product of high purity. We have developed a procedure for synthesizing amorphous BN that involves an explosive reaction between *B*-trichloroborazine and cesium metal initiated at 125°C in the absence of a solvent; HCl, H_2, and CsCl are also formed (*3*).

After removal of the by-products (*3*), x-ray powder diffraction patterns (*4*) and SEM images (*4*) reveal the amorphous nature of the BN product. Heating to 1100°C under vacuum for 24 hours converts it to the turbostratic phase. X-ray powder data are in accord with those in the literature for turbostratic BN (*1*), with increased resolution of the [002] reflection at 3.56 Å and the appearance of a broad peak corresponding to the [10] reflection (unresolved [100] and [101] reflections for hexagonal BN) at 2.13 Å.

Density measurements performed on the BN after the 1100°C heating step give a value of 1.7 g/cm^3, in reasonable accord with previously published data (*5*). The infrared spectrum of the turbostratic product is in agreement with published data (Fig. 1) (*6*). Electron energy loss spectroscopy (EELS) (*4*) reveals a B:N ratio of 1.00:1.06 (48.4 ± 0.3% to 51.6 ± 0.8%

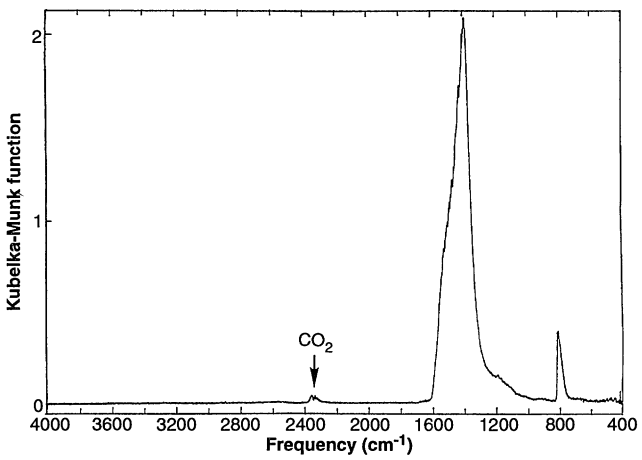

Fig. 1. Diffuse reflectance infrared spectrum of turbostratic BN.